

Where the Electron Correlation Energy resides within Hartree-Fock Theory

Itai Panas¹

¹Department of Chemistry and Chemical Engineering Division of Energy and Materials, Chalmers University of Technology, Environmental Inorganic chemistry unit

January 27, 2023

Where the Electron Correlation Energy resides within Hartree-Fock Theory

By

Itai Panas

Chalmers University of Technology

Department of Chemistry and Chemical Engineering

Division of Energy and Materials, Environmental Inorganic chemistry unit.

Abstract

A method for accurately estimating the electron correlation energy as a 1st order correction to the Hartree-Fock energy is presented. It succeeds by disallowing the representation of the electron repulsion operator to be more fine-grained than the corresponding representation of the two-particle density. To extract the electron correlation contribution to the molecular internal energy from the exact wavefunction, the short-range contribution to the electron repulsion operator is replaced by a corresponding correlation kinetic energy penalty. Utilizing the virial theorem, this self-interaction-free exact-exchange method becomes applicable on condition of stability of the Self-Consistent Field wave function. Laplace as well as Fourier transforms are resorted to as consistency checks. Atomic and small molecular ions are considered for validation. The latter require modelling of the screened Coulomb hole associated with 1s electrons owing to coupled short-range electron-nucleus and electron-electron interactions. For this purpose, Hooke's atom is analyzed ($0.03 \leq \omega \leq 1000$) and consistency is demonstrated for $1s^2$ Helium-like ions ($Z=1-36$). While impacting core-valence interactions, the said screening is absent in the valence as confirmed by the Be-like ions ($Z=3-36$) $1s^2 2s^2$ systems, for LiH, BeH⁺, Li₂ and for LiBe⁺. A chemistry associated exclusively with K-shell orbitals is briefly discussed based mainly on results for HeH⁺ and H₃⁺. Fractional charges scaling the Coulomb hole is inferred to better represent the complex correlation hole in hydrogen clusters and high-pressure metallic hydrogen.

1. Introduction

Any attempt at disentangling the electron correlation contributions to the many-electrons wave function must necessarily reflect on related assumptions in quantum theory as well as on the relevance for present-days electronic structure-based computational approaches. Soon it will be 100 years since Schrödinger's famous discovery of the equation that bears his name [1]. As validated by describing the hydrogen atom, its indelible impact on contemporary chemistry and physics, still today, is a tribute to its universality. It assumes quantum reality to be intertwined with classical mechanics via the Hamilton principal function that relates the coordinates and conjugated moments of a system's constituents to its internal energy via Hamilton-Jacobi equation. For a non-relativistic electron associated with a fixed proton, the time-independent Hamiltonian reduces to

$$H\left(q, \frac{dS}{q}\right) = E. \quad (1)$$

Here, the second essential *ad hoc* assumption is made. It concerns the classical action S taking the form

$$S = K \ln \psi \quad (2)$$

Upon inserting Eq. 2 into Eq.1 and subjecting it to the variational method, an equation is sought for the function ψ such that continuity and finiteness constraints on ψ as well as its derivatives are satisfied. The Schrödinger equation (SE) follows,

$$\Delta \psi + \frac{2m_e}{|K|^2} \left(E + \frac{e^2}{r} \right) \psi = 0. \quad (3)$$

$|K| = \hbar$ emerges, and the observed electronic spectrum of the hydrogen atom is deduced. It is truly remarkable how an analytical expression for the exact energy of a real system emerges, such that it implicitly complies with the Heisenberg indeterminacy principle in position and momentum of the electron [2]. The emergence of exact physical properties from probability functions, albeit for stationary states, through mathematical forms that remind of entropy was

explored by von Neumann [3] and later transferred into information theory by Shannon [4]. A crucial step in realizing the versatile potential of the single-electron SE was its independent-electrons generalization as developed by Hartree, Slater, Gaunt [5-7], and Slater and Fock [8,9]. The self-consistent field method was designed by Hartree to produce solutions to the resulting Hartree-Fock equations [10] that approximate the solution to one many-electron Schrödinger equation by those of many coupled one-electron integro-differential equations. The computability, however cumbersome at the time, was realized by Roothaan [11] by recasting the Hartree-Fock equations on the form of a matrix equation that is reiterated here for completeness. Thus, linear-combinations \mathbf{C} of basis functions belonging to a set $\{g\}$ are taken to represent the spatial components of the molecular orbitals

$$\phi_i = \sum_{\mu} c_{i\mu} g_{\mu} \quad (4)$$

such that \mathbf{C} is determined variationally upon minimizing the energy while constrained by maintaining orthonormal orbitals. The Hartree-Fock-Roothaan - method implies iteratively solving for

$$\mathbf{FC} = \mathbf{SC}\epsilon. \quad (5)$$

where the Fock matrix \mathbf{F} is a functional of \mathbf{C} . For doubly occupied space orbitals, the overlap matrix \mathbf{S} , and the Fock matrix \mathbf{F} take their well-known explicit forms

$$S_{\mu\nu} = \langle \mu | \nu \rangle \quad (6)$$

$$F_{\mu\nu} = \left\langle \mu \left| -\frac{1}{2}\nabla_1^2 - \sum_N \frac{Z_N}{|\mathbf{r}_1 - \mathbf{R}_N|} \right| \nu \right\rangle + \sum_{\gamma\delta} D_{\gamma\delta} \left\{ \langle \mu\gamma | \frac{1}{r_{12}} | \nu\delta \rangle - \frac{1}{2} \langle \mu\gamma | \frac{1}{r_{12}} | \delta\nu \rangle \right\} \quad (7)$$

Such that \mathbf{D} is the density matrix defined as

$$D_{\gamma\delta} = 2 \sum_{i=1}^{n_{el}/2} c_{i\gamma} c_{i\delta} \quad (8)$$

and

$$E_{HF} = \sum_{\mu\nu} D_{\mu\nu} \left[F_{\mu\nu} - \frac{1}{2} \sum_{\gamma\delta} D_{\gamma\delta} \left\{ \langle \mu\gamma | \frac{1}{r_{12}} | \nu\delta \rangle - \frac{1}{2} \langle \mu\gamma | \frac{1}{r_{12}} | \delta\nu \rangle \right\} \right] \quad (9)$$

A tribute to this handy *ab initio* formalism is that it is laying bare its own shortcomings. Thus, it was immediately realized that its usefulness would be limited by lack of electron correlation. Clearly, solutions to the Schrödinger equation for independent electrons are incompatible with the pairwise electron-electron interactions $\frac{1}{r_{12}}$ appearing in the *ab initio* Hamiltonian. Löwdin [12] introduced the definition

$$E_{corr} = E_{exact} - E_{HF} \quad (10)$$

Increased complexity in the wave function to include explicit inter-electronic distances in the wave function ansatz, as introduced by Hylleraas [13], offered a remedy. Generalization of the HF method by the configuration interaction CI approach was also shown to solve the electron correlation deficit in the HF formalism [14]. Hybrids of the two approaches have proven viable albeit still associated with high computational costs [15,16]. Vast amount of research went into clarifying what was missing and formulating intuitive remedies that completely or partially bypass the computational efforts associated with the enhanced complexity of the wave function ansatz [17,18]. Among these, density functional theory has emerged as the most successful one. What rendered DFT unique was how intuition was recast into theorems, establishing the connection between the ground state electron density, the ground state wavefunction, and the external potential [19] that paved the way for its practical realization. While resorting to the Slater determinant to provide the electron density, a set of equations, the Kohn Sham equations [20] analogous to the Hartree-Fock equations were formulated. Crucially retaining the kinetic energy expression for non-interacting electrons, KS DFT effectively replaces the HF exchange term by a universal exchange-correlation potential in the form of a functional of the electron density. This warrants computability for virtually all of chemistry and a large part of physics.

Today, approximate functionals are parametrized to satisfy a set of exact properties of the exact functional. A central characteristic of present days DFT is flexibility in design of new functionals. Yet, ambiguity in choice of functional, or tailoring it to fit a particular problem, may become a double-edged sword. Arguably, the need for quantitative 1st principles computability to complement experiment risk developing mainstream apologetic tolerance to flaws in the DFT methodology. Our exploratory contribution in this context is to unravel hidden conceptual robustness in bridging between HF and DFT [21] as well as between the Complete Active Space Self-Consistent Field and ensemble-DFT approaches [22,23]. In what follows, we summarize and extend on the former.

Surely, it is the exact definition of electron correlation as formulated in Eq. 10 that motivates revisiting the sources. To make progress, inspiration is drawn from three such sources. For one, the success of DFT is undeniable. Second, is the under-explored opportunity to utilize the Heisenberg indeterminacy principle beyond merely as a property of the exact wave function, in designing more efficient *ab initio* computational tools. Third, is the exact expression for the wave function from coupled-cluster theory [25,26] – the exponential operator $e^{\hat{T}}$ generating virtual excitations from the reference Slater determinant Ψ_{SD} with amplitudes determined by the coupled-cluster equations, such that

$$\begin{aligned} E_{exact}\langle\Psi|\Psi\rangle &= \langle\Psi|\hat{H}|\Psi\rangle = \langle\Psi_{SD}|e^{-\hat{T}}\hat{H}e^{\hat{T}}|\Psi_{SD}\rangle = \langle\Psi_{SD}|\hat{H}_{effective}|\Psi_{SD}\rangle \\ &= E_{exact}\langle\Psi_{SD}|\Psi_{SD}\rangle \end{aligned} \quad (11)$$

It is in this spirit that an expression for the electron correlations dressed Hamilton operator $\hat{H}_{effective}$, i.e., one that achieves the disentanglement of the exact electronic wave function into that of independent electrons, is justified and validated. And rather than cluster expansions of the wave function, we should anticipate additional terms in the electrons interaction representation to match the independent-electrons wave function. Intuitively, incorporation of indeterminacy of relative pair-wise electrons positions and relative pair-wise

electrons momenta in $\hat{H}_{effective}$ is sought. We will find that, to the extent that inter-electronic positions are correlated in the true electronic wave function, i.e., the one that matches the true non-relativistic Hamilton operator, their contribution to the internal energy may be readily disentangled at the Hartree-Fock level of theory by a virial augmented regularized electron repulsion operator. A most remarkable property of quantum theory is indeed its interplay with classical mechanics, underscoring its indelible role in the emerging quantum mechanics, cf. Eq. 1. The fact that the time-independent Schrödinger equation obeys the virial theorem was demonstrated, e.g., by Slater [28], and it has become ubiquitous in quantum chemistry, see for example [12,29]. While to some extent analogous to DFT [30], here, self-interaction-free disentanglement is offered that separates the exchange and correlation contributions to the exchange-correlation potential. It is found that the representation of the electron repulsion operator cannot be more fine-grained than the representation of the two-particle density.

In what follows, *Section 2* develops and assesses the general expressions utilized, *Section 3* deduces the coulomb hole augmented electron repulsion integrals (ERI:s), *Section 4* explores screening effects on the Coulomb hole by computing the correlation energies for (a) Hooke's atom $0.03 \leq \omega \leq 1000$ and (b) He-like ions ($Z=1-36$), *Section 5* partitions the density matrix to account for screening of the Coulomb hole in the 1s region owing to the singular electron-nucleus attractions, *Section 6* validates the partitioning and screening for Be-like (4 electrons) ions, while *Section 7* provides further proof of concept by computing total energies in the Hartree-Fock limit and corresponding correlation energy contributions for small molecular ions including 2-, 4-, and 6- electrons, and comparing those with exact numbers in the literature.

2. The Coulomb hole and its virial

In conventional wavefunction based *ab initio* quantum chemistry, electron correlation comprises a property of an increasingly complex wave function. It may be understood to describe a relative pairwise displacement of electrons to avoid highly repulsive regions in pair-space owing to the inter-electronic $\frac{1}{r_{12}}$ interaction. To achieve the effect of the said pairwise displacements, while remaining true to the independent particle ansatz, a Coulomb hole approach, referred to as the *regularized* Hartree-Fock method (reg-HF), where the correlation kinetic energy becomes absorbed in the coulomb and exchange potentials is reiterated and explored further below. Appropriately, we start out with exact expression for the electron repulsion energy in terms of the two-particle density $\rho_2(\mathbf{r}_1, \mathbf{r}_2)$

$$V_{ee} = \iint \frac{\rho_2(\mathbf{r}_1, \mathbf{r}_2)}{r_{12}} d^3\mathbf{r}_1 d^3\mathbf{r}_2 = \frac{1}{2} \iint \rho(\mathbf{r}_1)\rho(\mathbf{r}_2) \frac{1}{r_{12}} [1 + h^{xc}(\mathbf{r}_1, \mathbf{r}_2)] d^3\mathbf{r}_1 d^3\mathbf{r}_2 \quad (12)$$

By (i) factorizing $1 + h^{xc}(\mathbf{r}_1, \mathbf{r}_2) = (1 + h^x(\mathbf{r}_1, \mathbf{r}_2))(1 + h^c(|\mathbf{r}_1 - \mathbf{r}_2|))$ to account for non-local and interactions separately, (ii) replacing the exact electron density ρ by ρ_s referring here to the Slater determinantal wave function, and (iii) introducing the effective Coulomb hole attenuated electron-electron interaction operator $\langle G(r_{12}) \rangle$, Eq. 12 becomes reshaped into

$$V_{ee} = \frac{1}{2} \iint \rho_s(\mathbf{r}_1)\rho_s(\mathbf{r}_2) \langle G(r_{12}) \rangle [1 + h^x(\mathbf{r}_1, \mathbf{r}_2)] d^3\mathbf{r}_1 d^3\mathbf{r}_2 \quad (13)$$

where

$$\langle G(r_{12}) \rangle = \left\langle \frac{1}{r_{12}} [1 + h^c(|\mathbf{r}_1 - \mathbf{r}_2|)] \right\rangle \quad (14)$$

By virtue of Eqs. 13 and 14, the formalism to follow becomes self-interaction free. The \langle brackets \rangle are introduced to emphasize the effective nature of the operator thereby matching the truncated wave function $|\Psi_{SD}\rangle$. Thus, the sought Coulomb hole potential takes the form

$$\langle \hat{V}_{hole}^{dressed} \rangle = \left\langle \frac{h^c(|\mathbf{r}_1 - \mathbf{r}_2|)}{r_{12}} \right\rangle \quad (15)$$

To arrive at a practical expression for $\langle \hat{V}_{hole}^{dressed} \rangle$ the exact integral representation of $\frac{1}{r_{12}}$ is

partitioned according to

$$\frac{1}{r_{12}} = \frac{2}{\sqrt{\pi}} \int_0^\chi e^{-s^2 r_{12}^2} ds + \frac{2}{\sqrt{\pi}} \int_\chi^\infty e^{-s^2 r_{12}^2} ds \quad (16)$$

Subsequently, we identify

$$\langle \hat{V}_{hole}^{bare} \rangle_\chi = -\frac{2}{\sqrt{\pi}} \langle \int_\chi^\infty e^{-s^2 r_{12}^2} ds \rangle. \quad (17)$$

By virtue of the virial theorem but also considering that $\frac{1}{2} \mathbf{r}_{12} \cdot \nabla$ constitutes a pairwise displacement operator, it was noted in [21] that a consecutive regularization of $\frac{2}{\sqrt{\pi}} \int_\chi^\infty e^{-s^2 r_{12}^2} ds$ most generally leads to

$$\frac{2}{\sqrt{\pi}} \langle \int_\chi^\infty e^{-s^2 r_{12}^2} ds \rangle \approx \frac{2}{\sqrt{\pi}} \chi e^{-\chi^2 \theta r_{12}^2}; \quad r_{12} \neq 0. \quad (18)$$

This in turn implies that

$$\left\langle \frac{1}{r_{12}} \right\rangle \approx \frac{2}{\sqrt{\pi}} \int_0^\chi e^{-s^2 r_{12}^2} ds + \frac{2}{\sqrt{\pi}} \chi e^{-\chi^2 \theta r_{12}^2} \quad (19)$$

To estimate θ we first Fourier transform Eq. 19

$$\left\langle \sqrt{\frac{2}{\pi}} \frac{1}{k^2} \right\rangle \approx \sqrt{\frac{2}{\pi}} \frac{e^{-\frac{k^2}{4\chi^2}}}{k^2} + \frac{1}{\sqrt{2\pi}} \frac{e^{-\frac{k^2}{4\theta\chi^2}}}{\theta^{\frac{3}{2}} \chi^2} \quad (20)$$

We note that for $\chi^2 \gg k^2$ Eq. 20 reduces to

$$\sqrt{\frac{2}{\pi}} \frac{k^2}{4\chi^2} = \frac{1}{\sqrt{2\pi}} \frac{k^2}{\theta^{\frac{3}{2}} \chi^2} \quad (21)$$

so that

$$\theta = 2^{\frac{2}{3}} \approx 1.5874 \quad (22)$$

Assume the original time-independent Hartree-Fock theory to produce the Ψ_{SD} in the sense of Eq.11, so that ρ_s in Eq. 13 refers to independent electrons. The inferred stability of the time-independent solution implies that upon introducing $\langle \hat{V}_{hole}^{bare} \rangle_\chi$, the virial theorem must be obeyed to satisfy the requirement of being an *a priori* stable system. We write

$$\langle \hat{V}_{hole}^{dressed} \rangle_\chi = \langle \hat{V}_{hole}^{bare} \rangle_\chi - \langle \hat{T}_{corr} \rangle_\chi \quad (23)$$

Here, by virtue of this theorem, the implicit kinetic energy associated with the electron correlation becomes

$$\langle \hat{T}_{corr} \rangle_\chi = \langle -\frac{1}{2} \mathbf{r}_{12} \cdot \nabla \hat{V}_{hole}^{bare} \rangle_\chi \quad (24)$$

We proceed by inserting Eq.18 into Eq.24 to obtain

$$\langle \hat{T}_{corr} \rangle_\chi = \frac{2}{\sqrt{\pi}} \langle -\frac{1}{2} \mathbf{r}_{12} \cdot \nabla \int_\chi^\infty e^{-s^2 r_{12}^2} ds \rangle \approx \frac{2}{\sqrt{\pi}} \chi^3 \theta r_{12}^2 e^{-\chi^2 \theta r_{12}^2} \quad (25)$$

Thus, we arrive at the explicit expression, albeit parametrized by the cut-off χ (to be determined below), i.e.,

$$\begin{aligned} \langle G(r_{12}; \chi) \rangle &= \frac{1}{r_{12}} - \langle \hat{V}_{hole}^{dressed} \rangle_\chi \approx \frac{2}{\sqrt{\pi}} \int_0^\chi e^{-s^2 r_{12}^2} ds + \frac{2}{\sqrt{\pi}} \chi^3 \theta r_{12}^2 e^{-\chi^2 \theta r_{12}^2} \\ &\approx \frac{1}{r_{12}} - \frac{2}{\sqrt{\pi}} \chi e^{-\chi^2 \theta r_{12}^2} + \frac{2}{\sqrt{\pi}} \chi^3 \theta r_{12}^2 e^{-\chi^2 \theta r_{12}^2} \quad (26) \end{aligned}$$

and its Fourier transform

$$F \left(\frac{2}{\sqrt{\pi}} \int_0^\chi e^{-s^2 r_{12}^2} ds + \frac{2}{\sqrt{\pi}} \chi^3 \theta r_{12}^2 e^{-\chi^2 \theta r_{12}^2} \right) = \sqrt{\frac{2}{\pi}} \frac{e^{-\frac{k^2}{4\chi^2}}}{k^2} + \frac{1}{\sqrt{2\pi} \theta^{\frac{3}{2}} \chi^2} \left[\frac{3}{2} - \frac{k^2}{4\theta \chi^2} \right] e^{-\frac{k^2}{4\theta \chi^2}} \quad (27)$$

The terms that enter Eqs. 26 and 27 are plotted in Figure 1. In particular, Equation 26

replaces the intuitive soft Coulomb hole expression $\frac{1-e^{-\omega r_{12}^2}}{r_{12}}$ in [18].

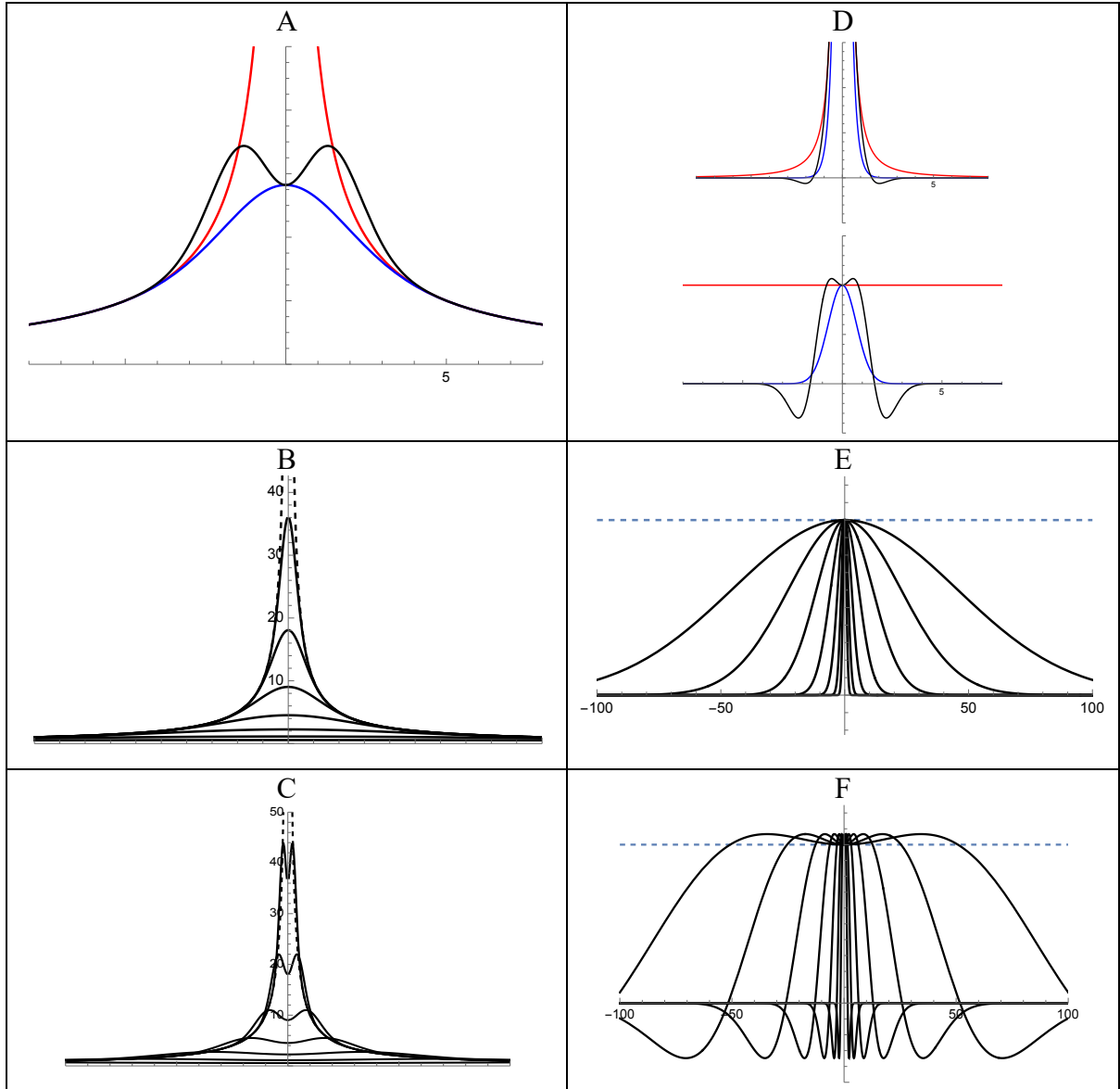


Figure 1.

A. The three functions of r_{12} , cf. Eq.26, corresponding to $\frac{1}{r_{12}}$ (red), $\frac{2}{\sqrt{\pi}} \int_0^\chi e^{-s^2 r_{12}^2} ds$ (blue), and $\frac{2}{\sqrt{\pi}} \int_0^\chi e^{-s^2 r_{12}^2} ds + \frac{2}{\sqrt{\pi}} \chi^3 \theta r_{12}^2 e^{-\chi^2 \theta r_{12}^2}$ (black), $\chi = 0.5$, $\theta = 2^{\frac{2}{3}}$. **B.** The regularized coulomb interaction $\frac{2}{\sqrt{\pi}} \int_0^\chi e^{-s^2 r_{12}^2} ds$ for χ : 0.5, 1, 2, 4, 8, 16, 32. Dashed is $\frac{1}{r_{12}}$. **C.** The virial augmented regularized coulomb interaction $\frac{2}{\sqrt{\pi}} \int_0^\chi e^{-s^2 r_{12}^2} ds + \frac{2}{\sqrt{\pi}} \chi^3 \theta r_{12}^2 e^{-\chi^2 \theta r_{12}^2}$ for χ : 0.5, 1, 2, 4, 8, 16, 32. Dashed is $\frac{1}{r_{12}}$. **D.** Top: Fourier transforms of (A): $F\left(\frac{1}{r_{12}}\right) = \sqrt{\frac{2}{\pi}} \frac{1}{k^2}$ (Red), $F\left(\frac{2}{\sqrt{\pi}} \int_0^\chi e^{-s^2 r_{12}^2} ds\right) = \sqrt{\frac{2}{\pi}} \frac{e^{-\frac{k^2}{4\chi^2}}}{k^2}$ (Blue), and $F\left(\frac{2}{\sqrt{\pi}} \int_0^\chi e^{-s^2 r_{12}^2} ds + \frac{2}{\sqrt{\pi}} \chi^3 \theta r_{12}^2 e^{-\chi^2 \theta r_{12}^2}\right) = \sqrt{\frac{2}{\pi}} \frac{e^{-\frac{k^2}{4\chi^2}}}{k^2} + \frac{1}{\sqrt{2\pi}\theta^{\frac{3}{2}}\chi^2} \left[\frac{3}{2} - \frac{k^2}{4\theta\chi^2}\right] e^{-\frac{k^2}{4\theta\chi^2}}$ (Black). $\theta = 2^{\frac{2}{3}}$, $\chi = 0.5$. Bottom: same as Top, scaled by $\sqrt{\frac{2}{\pi}} k^{-2}$. Dashed is $F\left(\frac{1}{r_{12}}\right) / \sqrt{\frac{2}{\pi}} k^{-2} = 1$. **E.** Fourier transforms of (B) scaled by $\sqrt{\frac{2}{\pi}} k^{-2}$. Dashed is $F\left(\frac{1}{r_{12}}\right) / \sqrt{\frac{2}{\pi}} k^{-2} = 1$. **F.** Fourier transforms of (C) scaled by $\sqrt{\frac{2}{\pi}} k^{-2}$. Dashed is $F\left(\frac{1}{r_{12}}\right) / \sqrt{\frac{2}{\pi}} k^{-2} = 1$.

3. The Coulomb hole in a 4-center Gaussian representation

– *identifying the cut-of* $\chi_{\gamma\delta}^{\mu\nu}$

In as much as the gaussian probability density function maximizes the information entropy for a given variance in the data, it is utilized here to construct an *a priori* unbiased gauge for the electron correlation. Moreover, spanning the molecular orbitals in a gaussian basis set $\{\{\Gamma_{\mu}(\mathbf{r}_1)\}\}$ indeed implies spanning the electron density in the corresponding product space $\{\{\Gamma_{\mu}(\mathbf{r}_1)\} \otimes \{\Gamma_{\nu}(\mathbf{r}_1)\}\} \Rightarrow \{\{\Gamma_{\mu\nu}(\mathbf{r}_1)\}\}$. This by virtue of the gaussian product theorem. Here, the basis for spanning the two-particle density comprises $\{\{\Gamma_{\mu\nu}(\mathbf{r}_1)\} \otimes \{\Gamma_{\gamma\delta}(\mathbf{r}_2)\}\}$ while the pair-correlation function becomes absorbed by the effective electron-electron interaction $G(r_{12}; \chi_{\gamma\delta}^{\mu\nu})$. Thus, implementation of the novel Coulomb hole attenuated electron repulsion operator Eq. 26 in the matrix representation of the Hartree-Fock equations for a gaussian basis sets requires rewriting the ERI “metric” for the Coulomb and exchange contributions to the electron repulsion energy according to

$$\begin{aligned} V_{ee} &= \iint \frac{\rho_2(\mathbf{r}_1, \mathbf{r}_2)}{r_{12}} d^3\mathbf{r}_1 d^3\mathbf{r}_2 \\ &\approx \frac{1}{2} \sum_{\mu\nu} \sum_{\gamma\delta} D_{\mu\nu} D_{\gamma\delta} \left\{ \langle \mu\gamma | \langle G(r_{12}; \chi_{\gamma\delta}^{\mu\nu}) | \nu\delta \rangle \right. \\ &\quad \left. - \frac{1}{2} \langle \mu\gamma | \langle G(r_{12}; \chi_{\gamma\delta}^{\mu\nu}) | \delta\nu \rangle \right\} \quad (28) \end{aligned}$$

In what follows, we will use the short-hand notation $\langle \mu\gamma | \langle G(r_{12}; \chi_{\gamma\delta}^{\mu\nu}) | \nu\delta \rangle \equiv$

$\langle\langle G(r_{12}; \chi_{\gamma\delta}^{\mu\nu}) \rangle\rangle_{\gamma\delta}^{\mu\nu}$ to represent the attenuated ERI:s, such that

$$\begin{aligned} \langle\langle G(r_{12}; \chi_{\gamma\delta}^{\mu\nu}) \rangle\rangle_{\gamma\delta}^{\mu\nu} \\ \approx \langle \frac{1}{r_{12}} \rangle_{\gamma\delta}^{\mu\nu} - \frac{2}{\sqrt{\pi}} \langle\langle \chi_{\gamma\delta}^{\mu\nu} e^{-\chi_{\gamma\delta}^{\mu\nu 2} \theta r_{12}^2} \rangle\rangle_{\gamma\delta}^{\mu\nu} + \frac{2}{\sqrt{\pi}} \langle\langle \chi_{\gamma\delta}^{\mu\nu 3} \theta r_{12}^2 e^{-\chi_{\gamma\delta}^{\mu\nu 2} \theta r_{12}^2} \rangle\rangle_{\gamma\delta}^{\mu\nu} \quad (29) \end{aligned}$$

and correspondingly for $\langle\langle G(r_{12}; \chi_{\gamma\nu}^{\mu\delta}) \rangle\rangle_{\gamma\nu}^{\mu\delta}$. In bypassing, it is noted that Eq. 29 may equivalently be written as

$$\langle\langle G(r_{12}; \chi_{\gamma\delta}^{\mu\nu}) \rangle\rangle_{\gamma\delta}^{\mu\nu} \approx \frac{2}{\sqrt{\pi}} \langle\langle \int_0^{\chi_{\gamma\delta}^{\mu\nu}} e^{-s^2 r_{12}^2} ds \rangle\rangle_{\gamma\delta}^{\mu\nu} + \frac{2}{\sqrt{\pi}} \langle\langle \chi_{\gamma\delta}^{\mu\nu 3} \theta r_{12}^2 e^{-\chi_{\gamma\delta}^{\mu\nu 2} \theta r_{12}^2} \rangle\rangle_{\gamma\delta}^{\mu\nu} \quad (30)$$

Thus, the regularized Hartree-Fock approach is realized in the conventional framework as follows: Let $\mathbf{A}_\mu, \mathbf{A}_\nu, \mathbf{A}_\gamma$ and \mathbf{A}_δ be origins of gaussian basis functions with corresponding exponents $\alpha_\mu, \alpha_\nu, \alpha_\gamma$ and α_δ . In what follows, we limit ourselves to s-type basis functions and include ghost functions to mimic the effects of atom-centered polarization functions. Let

$$\mathbf{P} = \frac{\alpha_\mu \mathbf{A}_\mu + \alpha_\nu \mathbf{A}_\nu}{\alpha_\mu + \alpha_\nu} \quad (31)$$

$$\mathbf{Q} = \frac{\alpha_\gamma \mathbf{A}_\gamma + \alpha_\delta \mathbf{A}_\delta}{\alpha_\gamma + \alpha_\delta} \quad (32)$$

$$R_{PQ}^2 = |\mathbf{P} - \mathbf{Q}|^2 \quad (33)$$

$$S_{\mu\nu} = \left(\frac{4\alpha_\mu\alpha_\nu}{(\alpha_\mu + \alpha_\nu)^2} \right)^{3/4} \exp \left[-\frac{\alpha_\mu\alpha_\nu}{\alpha_\mu + \alpha_\nu} (\mathbf{A}_\mu - \mathbf{A}_\nu)^2 \right] \quad (34)$$

where $S_{\mu\nu}$ and correspondingly $S_{\gamma\delta}$ constitute the usual overlap integrals over gaussian functions. Introducing

$$\kappa = \alpha_\mu + \alpha_\nu \quad (35)$$

$$\xi = \alpha_\gamma + \alpha_\delta \quad (36)$$

$$\beta = \frac{\kappa \cdot \xi}{\kappa + \xi} \quad (37)$$

we obtain the well-known expression

$$\langle\langle \frac{1}{r_{12}} \rangle\rangle_{\gamma\delta}^{\mu\nu} = S_{\mu\nu} S_{\gamma\delta} \frac{\pi^3}{(\kappa \cdot \xi)^{3/2}} 2 \left(\frac{\beta}{\pi} \right)^{1/2} F_0(\beta \cdot R_{PQ}^2) \quad (38)$$

where

$$F_0(W) = \int_0^1 e^{-Ws^2} ds \quad (39)$$

An expression for χ is obtained by merging the generic Eq. 19 into Eq 38

$$\left\langle \frac{1}{r_{12}} \right\rangle_{\gamma\delta}^{\mu\nu} \approx \left\langle \frac{2}{\sqrt{\pi}} \int_0^{\chi_{\gamma\delta}^{\mu\nu}} e^{-s^2 r_{12}^2} ds \right\rangle_{\gamma\delta}^{\mu\nu} + \left\langle \frac{2}{\sqrt{\pi}} \chi_{\gamma\delta}^{\mu\nu} e^{-\chi_{\gamma\delta}^{\mu\nu 2} \theta r_{12}^2} \right\rangle_{\gamma\delta}^{\mu\nu} \quad (40)$$

On expanding Eq. 40 to 1st order in R_{PQ}^2 and identifying terms we obtain

$$\chi_{\gamma\delta}^{\mu\nu 2} = a \cdot \beta \quad (41)$$

$$a = -\frac{1}{2} + \frac{\sqrt{5}}{2} \approx 0.6180 \quad (42)$$

$$\theta = 1 + \frac{\sqrt{5}}{3} \approx 1.7454 \quad (43)$$

Equation 41 is the sought expression that constrains the representation of the interaction so that it cannot be more fine-grained than the corresponding representation of the two-particle density. Besides the sought cut-off $\chi_{\gamma\delta}^{\mu\nu}$, an alternative expression for θ , previously obtained by the complementary Fourier transformation procedure, cf. Eqs. 20-22, emerges. A comparison between the different impacts that the two values of θ have on Eq. 40, is shown in Figure 2.

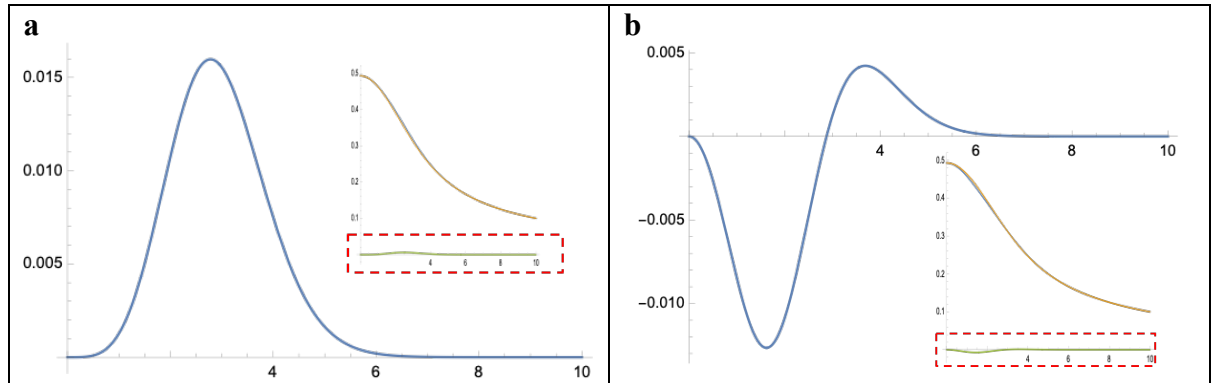


Figure 2. Assessments of Eq. 40 as function of R_{PQ} . $\left\langle \frac{1}{r_{12}} \right\rangle_{\gamma\delta}^{\mu\nu}$ and $\left\langle \frac{2}{\sqrt{\pi}} \int_0^{\chi_{\gamma\delta}^{\mu\nu}} e^{-s^2 r_{12}^2} ds \right\rangle_{\gamma\delta}^{\mu\nu} + \left\langle \frac{2}{\sqrt{\pi}} \chi_{\gamma\delta}^{\mu\nu} e^{-\chi_{\gamma\delta}^{\mu\nu 2} \theta r_{12}^2} \right\rangle_{\gamma\delta}^{\mu\nu}$ are superimposed in insets. Errors in dashed red frames are enlarged.
(a) relative error for $\theta = 1 + \frac{\sqrt{5}}{3}$ - from Eq. 40 developed to 1st order in R_{PQ}^2 .
(b) relative error for $\theta = \frac{2}{3}$ - from Fourier transform of Eq. 19, expanded to 1st order in $\frac{k^2}{4\chi^2}$, and inserted in Eq. 40.

We obtain

$$\left\langle \frac{2}{\sqrt{\pi}} \int_0^{\chi_{\gamma\delta}^{\mu\nu}} e^{-s^2 r_{12}^2} ds \right\rangle_{\gamma\delta}^{\mu\nu} = S_{\mu\nu} S_{\gamma\delta} \frac{\pi^3}{(\kappa \cdot \xi)^{3/2}} 2 \left(\frac{\beta}{\pi} \right)^{\frac{1}{2}} a \cdot F_0(a^2 \cdot \beta \cdot R_{PQ}^2) \quad (44)$$

$$\left\langle \frac{2}{\sqrt{\pi}} \chi e^{-\chi_{\gamma\delta}^{\mu\nu 2} \theta r_{12}^2} \right\rangle_{\gamma\delta}^{\mu\nu} = S_{\mu\nu} S_{\gamma\delta} \frac{\pi^3}{(\kappa \cdot \xi)^{3/2}} 2 \left(\frac{\beta}{\pi} \right)^{\frac{1}{2}} \cdot a^2 \cdot \exp(-a^2 \cdot \beta \cdot \theta \cdot R_{PQ}^2) \quad (45)$$

and

$$\begin{aligned} & \left\langle \frac{1}{2} \mathbf{r}_{12} \cdot \nabla \frac{2}{\sqrt{\pi}} \chi_{\gamma\delta}^{\mu\nu} e^{-\chi_{\gamma\delta}^{\mu\nu 2} \theta r_{12}^2} \right\rangle_{\gamma\delta}^{\mu\nu} \\ &= S_{\mu\nu} S_{\gamma\delta} \frac{\pi^3}{(\kappa \cdot \xi)^{3/2}} 2 \left(\frac{\beta}{\pi} \right)^{\frac{1}{2}} \\ & \cdot a^4 \left[\frac{3}{2} + a \cdot \beta \cdot \theta \cdot R_{PQ}^2 \right] \exp(-a^2 \cdot \beta \cdot \theta \cdot R_{PQ}^2) \end{aligned} \quad (46)$$

Thus, corresponding to Eq. 29, we obtain

$$\begin{aligned} \langle\langle G(r_{12}; \chi_{\gamma\delta}^{\mu\nu}) \rangle\rangle_{\gamma\delta}^{\mu\nu} &\approx S_{\mu\nu} S_{\gamma\delta} \frac{\pi^3}{(\kappa \cdot \xi)^{\frac{3}{2}}} \cdot 2 \left(\frac{\beta}{\pi} \right)^{\frac{1}{2}} \cdot \\ & \left[F_0(\beta \cdot R_{PQ}^2) - \left\{ a^2 - a^4 \left[\frac{3}{2} + a \cdot \beta \cdot \theta \cdot R_{PQ}^2 \right] \right\} \exp(-a^2 \cdot \beta \cdot \theta \cdot R_{PQ}^2) \right] \end{aligned} \quad (47)$$

while matching Eq. 30, we get

$$\begin{aligned} \langle\langle G(r_{12}; \chi_{\gamma\delta}^{\mu\nu}) \rangle\rangle_{\gamma\delta}^{\mu\nu} &\approx S_{\mu\nu} S_{\gamma\delta} \frac{\pi^3}{(\kappa \cdot \xi)^{\frac{3}{2}}} \cdot 2 \left(\frac{\beta}{\pi} \right)^{\frac{1}{2}} \cdot \\ & \left[a \cdot F_0(a^2 \cdot \beta \cdot R_{PQ}^2) + a^4 \left[\frac{3}{2} + a \cdot \beta \cdot \theta \cdot R_{PQ}^2 \right] \exp(-a^2 \cdot \beta \cdot \theta \cdot R_{PQ}^2) \right] \end{aligned} \quad (48)$$

Again, it follows from Eqs. 47 and 48 that

$$F_0(\beta \cdot R_{PQ}^2) \approx a \cdot F_0(a^2 \cdot \beta \cdot R_{PQ}^2) + a^2 \cdot \exp(-a^2 \cdot \beta \cdot \theta \cdot R_{PQ}^2) \quad (49)$$

Eq. 49 is analogous to Eq. 40, that was evaluated in Figure 2.

4. Scaled Coulomb hole from nuclear attraction screening

Equations 47 and 48 comprise the final expressions in cases where the electron-electron interaction is the only electron associated interaction that possesses a singularity, e.g., when Effective Core Potentials (ECP:s) are employed. In cases where the electron correlation for 1s electrons are computed, the impact of electron-nuclei interactions becomes to screen the Coulomb hole and increasingly so with increased nuclear charges. To account for this effect, we introduce a scaling factor f and write analogously to Eq. 47

$$\langle\langle G(r_{12}; \chi_{\gamma\delta}^{\mu\nu}) \rangle\rangle_{\gamma\delta}^{\mu\nu} \approx S_{\mu\nu} S_{\gamma\delta} \frac{\pi^3}{(\kappa \cdot \xi)^{\frac{3}{2}}} \cdot 2 \left(\frac{\beta}{\pi}\right)^{\frac{1}{2}} \cdot \left[F_0(\beta \cdot R_{PQ}^2) - f \left\{ a^2 - a^4 \left[\frac{3}{2} + a \cdot \beta \cdot \theta \cdot R_{PQ}^2 \right] \right\} \exp(-a^2 \cdot \beta \cdot \theta \cdot R_{PQ}^2) \right] \quad (50)$$

and corresponding to Eq. 48

$$\langle\langle G(r_{12}; \chi_{\gamma\delta}^{\mu\nu}) \rangle\rangle_{\gamma\delta}^{\mu\nu} \approx S_{\mu\nu} S_{\gamma\delta} \frac{\pi^3}{(\kappa \cdot \xi)^{\frac{3}{2}}} \cdot 2 \left(\frac{\beta}{\pi}\right)^{\frac{1}{2}} \cdot \left[a \cdot F_0(a^2 \cdot \beta \cdot R_{PQ}^2) + a^2 \cdot \exp(-a^2 \cdot \beta \cdot \theta \cdot R_{PQ}^2) - f \left\{ a^2 - a^4 \left[\frac{3}{2} + a \cdot \beta \cdot \theta \cdot R_{PQ}^2 \right] \right\} \exp(-a^2 \cdot \beta \cdot \theta \cdot R_{PQ}^2) \right] \quad (51)$$

The validity of these forms and the expression for the scaling factor is addressed in sections 4.a and 4.b.

4.a. *Scaling the Coulomb hole in Hooke's atom*

Here, we turn to Hooke's atom to validate the ansatz. This system has arguably become a gold standard for descriptions of electron correlation in two-electron systems, cf. [31-35]. For

this model system, the electron-nucleus attraction in Eq. 7 is replaced by a harmonic oscillator potential to produce

$$\hat{H} = -\frac{1}{2}(\nabla_1^2 + \nabla_2^2) + \frac{1}{2}\omega^2(r_1^2 + r_2^2) + \frac{1}{r_{12}} \quad (52)$$

On implementing the regularized Hartree-Fock (reg-HF) scheme to solve for Hooke's atom, it is first noted that Eqs. 50 and 51 reduce to

$$\langle G(r_{12}; \chi_{\gamma\delta}^{\mu\nu}) \rangle_{\gamma\delta}^{\mu\nu} = S_{\mu\nu} S_{\gamma\delta} \frac{\pi^3}{(\kappa \cdot \xi)^{\frac{3}{2}}} \cdot 2 \left(\frac{\beta}{\pi}\right)^{\frac{1}{2}} \left[1 - f \cdot \left(a^2 - \frac{3}{2}a^4\right) \right]$$

In line with the leading correction to the total energy of Hooke's atom at large ω being

$O(\omega^{-0.5})$ [34], two analogous forms, i.e., $f = \frac{1}{a^2 - \frac{3}{2}a^4 + \sqrt{\omega}}$ and $f = \frac{1}{\sqrt{(a^2 - \frac{3}{2}a^4)^2 + \omega}}$, are

considered here, both satisfying the requirement that non-interacting electrons result in the limit $\omega \rightarrow 0$. While indeed performing similarly for large ω , the former performs significantly better for intermediate and small ω . Therefore, only the results for

$$\langle\langle G(r_{12}; \chi_{\gamma\delta}^{\mu\nu}) \rangle\rangle_{\gamma\delta}^{\mu\nu} = S_{\mu\nu} S_{\gamma\delta} \frac{\pi^3}{(\kappa \cdot \xi)^{\frac{3}{2}}} \cdot 2 \left(\frac{\beta}{\pi}\right)^{\frac{1}{2}} \left[1 - \frac{1}{1 + \sqrt{\frac{\omega}{(a^2 - \frac{3}{2}a^4)^2}}} \right] \quad (54)$$

are provided in Table 1. Clearly, these results set the standard for the accuracy that is expected from the reg-HF approach.

Table 1. Hooke's atom energies from Hartree-Fock, regularized Hartree-Fock, $f = \frac{1}{a^2 - \frac{3}{2}a^4 + \sqrt{\omega}}$, are compared with Full CI and $\frac{E_{exact}}{\omega}$ results [34] for a range of different force constants.

ω	E_{HF}	E_{reg-HF}	E_{FCI}	$\frac{E_{reg-HF}}{\omega}$	$\frac{E_{exact}}{\omega}$
0.03	0.207816	0.187235	0.1872131	6.241165	6.240437
0.033	0.223300	0.202112	0.2020337	6.124777	6.122233
0.036	0.238511	0.216779	0.2166358	6.021639	6.017661
0.0365373	0.241209	0.219383	0.2192297	6.004370	6.000161
0.04	0.258422	0.236025	0.2358069	5.900625	5.895173
0.05	0.306693	0.282890	0.282503	5.657802	5.65006
0.06	0.353283	0.328342	0.3278107	5.472369	5.463512
0.08	0.442870	0.416165	0.4153963	5.202059	5.192454
0.1	0.529042	0.501005	0.5000511	5.010052	5.000511
0.15	0.734982	0.704637	0.7033557	4.697582	4.689038
0.2	0.932305	0.900425	0.8989284	4.502127	4.494642
0.3	1.311900	1.278022	1.2762559	4.260072	4.254186
0.4	1.679136	1.643962	1.6420337	4.109905	4.105084
0.5	2.038439	2.002332	2.0002946	4.004665	4.000589
1.	3.771464	3.732855	3.7305644	3.732855	3.730564
2.	7.101464	7.060903	7.0584674	3.530451	3.529234
5.	16.756755	16.714320	16.711796	3.342863	3.342359
10.	32.495528	32.452094	32.449546	3.245209	3.244955
100.	307.950844	307.905672	307.90313	3.079057	3.079031
1000.	3025.203196	3025.157450	3025.1549	3.025157	3.025155

4.b. *Scaling of the 1s Coulomb hole in Helium like ions*

Scaling of the Coulomb hole, by the force constant in case of Hooke's atom or by nuclear charge in case of Coulombic K-shell electron-nucleus attraction, respectively, may be taken to reflect their infinitely high parabolic potential walls and the infinitely deep electron-nucleus attraction wells. Similar asymptotic considerations as for Hooke's atom, albeit

replacing $\omega^{-0.5}$ by Z , see e. g. [12,34,35], lead to comparing $f_K = \frac{1}{\sqrt{(a^2 - \frac{3}{2}a^4)^2 + Z^2}}$ to $f_K =$

$\frac{1}{a^2 - \frac{3}{2}a^4 + Z}$. The former expression is found to outperform the latter for the low- Z systems,

while they behave similarly for the intermediate and high- Z systems. Thus, comparison

between experiment and reg-HF is provided in Table 2 for $f_K = \frac{1}{\sqrt{(a^2 - \frac{3}{2}a^4)^2 + Z^2}}$,

corresponding to

$$\langle\langle G(r_{12}; \chi_{\gamma\delta}^{\mu\nu}) \rangle\rangle_{\gamma\delta}^{\mu\nu} = S_{\mu\nu} S_{\gamma\delta} \frac{\pi^3}{(\kappa \cdot \xi)^{\frac{3}{2}}} \cdot 2 \left(\frac{\beta}{\pi}\right)^{\frac{1}{2}} \left[1 - \frac{1}{\sqrt{1 + \frac{Z^2}{(a^2 - \frac{3}{2}a^4)^2}}} \right] \quad (55)$$

Table 2. Comparison between Hartree-Fock and regularized Hartree-Fock for He-like 2-electron ions. $f_K = \frac{1}{\sqrt{(a^2 - \frac{3}{2}a^4)^2 + Z^2}}$, virtually Z -independent electron correlation energy is observed in agreement with experiment [36]. $Z=1$ is H. For discussion, see text. HGBS-9 basis set [37] is employed in this work.

Z	E_{HF}	E_{reg-HF}	$E_{HF} - E_{reg-HF}$	E_{corr} [29]
1	-0.48792973	-0.51976453	0.0318348	0.0407
2	-2.86167999	-2.90337214	0.0416922	0.0421
3	-7.23641519	-7.28125252	0.0448373	0.0435
4	-13.61129940	-13.65768997	0.0463906	0.0443
5	-21.98623441	-22.03355089	0.0473165	0.0448
6	-32.36119279	-32.40912403	0.0479312	0.0451
7	-44.73616385	-44.78453298	0.0483691	0.0453
8	-59.11114255	-59.15983941	0.0486969	0.0455
9	-75.48612621	-75.53507758	0.0489514	0.0456
10	-93.86111328	-93.910267100	0.0491547	0.0457
11	-114.23610277	-114.28542371	0.0493209	0.0458
12	-136.61109408	-136.66055340	0.0494593	0.0459
13	-160.98608675	-161.03566310	0.0495763	0.0459
14	-187.36108048	-187.41075707	0.0496766	0.046
15	-215.73607506	-215.78583849	0.0497634	0.0461
16	-246.11107032	-246.16090969	0.0498394	0.0461
17	-278.48606614	-278.53597250	0.0499064	0.0462
18	-312.86106242	-312.91102829	0.0499659	0.0463
19	-349.23605909	-349.28607820	0.0500191	0.0463
20	-387.61105607	-387.66112308	0.050067	0.0463
21	-427.98605334	-428.03616368	0.0501103	0.046

22	-470.36105085	-470.41120056	0.0501497	0.046
23	-514.73604855	-514.78623421	0.0501857	0.047
24	-561.11104645	-561.16126506	0.0502186	0.047
25	-609.48604449	-609.53629340	0.0502489	0.047
26	-659.86104268	-659.91131956	0.0502769	0.047
27	-712.23604097	-712.28634375	0.0503028	0.047
28	-766.61103940	-766.66136622	0.0503268	0.047
29	-822.98603791	-823.03638711	0.0503492	0.047
30	-881.36103650	-881.41140658	0.0503701	0.047
31	-941.73603516	-941.78642478	0.0503896	0.047
32	-1004.11103390	-1004.16144183	0.0504079	0.047
33	-1068.48603267	-1068.53645780	0.0504251	0.047
34	-1134.86103159	-1134.91147290	0.0504413	0.047
35	-1203.23603042	-1203.28648700	0.0504566	0.047
36	-1273.61102938	-1273.66150037	0.050471	0.047

5. Core-Valence separation

Thus, the parameters χ and θ , as well as the expression for the scaling f of the Coulomb hole in 1s have been determined, the latter owing to the singular electron-nucleus attraction [12].

To form the inter-electronic contribution to the Hartree-Fock energy, incorporation of Eq. 50 or Eq 51) in Eq. 9 requires partitioning of the density matrix \mathbf{D} into $\mathbf{D}^{inner} + \mathbf{D}^{outer}$ contributions

$$D_{\mu\nu}^{inner}(f_K) = 2 \sum_{i=1}^{K-shells} f_i c_{i\mu} c_{iv} \quad (56)$$

$$D_{\mu\nu}^{outer}(f_V) = 2 \sum_{i=K-shells+1}^{n_{el}/2} f_i c_{i\mu} c_{iv} \quad (57)$$

This way, the electron correlation energy takes the form

$$E_{corr} = \frac{1}{8} \sum_{\mu\nu} \sum_{\gamma\delta} \frac{2}{\sqrt{\pi}} \left\{ \langle \langle \chi e^{-\chi^2 \theta r_{12}^2} (1 - \chi^2 \theta r_{12}^2) \rangle \rangle_{\gamma\delta}^{\mu\nu} - \frac{1}{2} \langle \langle \chi e^{-\chi^2 \theta r_{12}^2} (1 - \chi^2 \theta r_{12}^2) \rangle \rangle_{\gamma\nu}^{\mu\delta} \right\} \\ \cdot (2D_{\mu\nu}^{inner}(f_K) D_{\gamma\delta}^{inner} + D_{\mu\nu}^{inner}(f_K) D_{\gamma\delta}^{outer} + D_{\mu\nu}^{outer} D_{\gamma\delta}^{inner}(f_K) \\ + 2D_{\mu\nu}^{outer}(f_V) D_{\gamma\delta}^{outer}) \quad (58)$$

It is noted that only the last term in Eq. 58 applies in case of ECP:s.

6. Validation I: Be-like $1s^2 2s^2$ ions

To validate the core-valence separation procedure we first turn to the Be-like ions, in that these possess both 1s (core) and 2s (valence) electrons, see Table 3. The results for $1s^2$ and $1s^2 2s^2$ ions are summarized in Figure 3, and some are highlighted further in Table. 4 for comparison with literature. It is noted that the scaled coulomb hole impacts exclusively interactions that involve K-shell orbitals, i.e., it vanishes for the 2s-2s valence interactions in Be-like ions, i.e., $f_V = 1$ in Eq. 58. In cases where ECP:s are resorted to, so that only valence electrons are described explicitly, then $f_V = f = 1$.

Table 3. Comparison between Hartree-Fock and regularized

Hartree-Fock energies for Be-like 4-electron ions. $f_K = \frac{1}{\sqrt{(a^2 - \frac{3}{2}a^4)^2 + Z^2}}$ and $f_V =$

1. Comparison with experiment [36] is provided. $Z=3$ is Li. HGBS-9 basis set [37] is employed in this work.

Z	E_{HF}	E_{reg-HF}	$E_{reg-HF} - E_{HF}$	E_{corr} [29]
3	-7.42820493	-7.49909271	-0.070887777	-0.07255 [33]
4	-14.57302313	-14.66640254	-0.093379404	-0.0944
5	-24.23757511	-24.34803802	-0.11046291	-0.1123
6	-36.40849520	-36.53415089	-0.12565569	-0.1268
7	-51.08231679	-51.22222815	-0.13991136	-0.1412
8	-68.25771031	-68.41133480	-0.15362450	-0.1551
9	-87.93405264	-88.10104541	-0.16699278	-0.1684
10	-110.11101216	-110.29113952	-0.18012736	-0.1814
11	-134.78839590	-134.98149183	-0.19309592	-0.1941
12	-161.96608375	-162.17202590	-0.20594215	-0.2066
13	-191.64399715	-191.86269272	-0.21869556	-0.219
14	-223.82208249	-224.05345935	-0.23137686	-0.2313
15	-258.50030183	-258.74430282	-0.24400098	-0.2435
16	-295.67862767	-295.93520668	-0.25657901	-0.2556
17	-335.35703957	-335.62615889	-0.26911931	-0.2677
18	-377.53552205	-377.81715041	-0.28162836	-0.2797
19	-422.21406303	-422.50817423	-0.29411120	-0.2917
20	-469.39265318	-469.69922504	-0.30657187	-0.3037

21	-519.07128480	-519.39029840	-0.31901359	-0.316
22	-571.24995205	-571.58139107	-0.33143902	-0.327
23	-625.92864995	-626.27250026	-0.34385031	-0.339
24	-683.10737426	-683.46362352	-0.35624927	-0.351
25	-742.78612187	-743.15475926	-0.36863739	-0.363
26	-804.96488973	-805.34590569	-0.38101596	-0.375
27	-869.64367570	-870.03706175	-0.39338605	-0.387
28	-936.82247741	-937.22822599	-0.40574858	-0.398
29	-1006.50129340	-1006.91939775	-0.41810435	-0.411
30	-1078.68012226	-1079.11057630	-0.43045404	-0.423
31	-1153.35896249	-1153.80176074	-0.44279825	-0.434
32	-1230.53781297	-1230.99295047	-0.45513750	-0.446
33	-1310.21667309	-1310.68414533	-0.46747224	-0.458
34	-1392.39554095	-1392.87534383	-0.47980288	-0.47
35	-1477.07441753	-1477.56654730	-0.49212976	-0.482
36	-1564.25330054	-1564.75775377	-0.50445323	-0.494

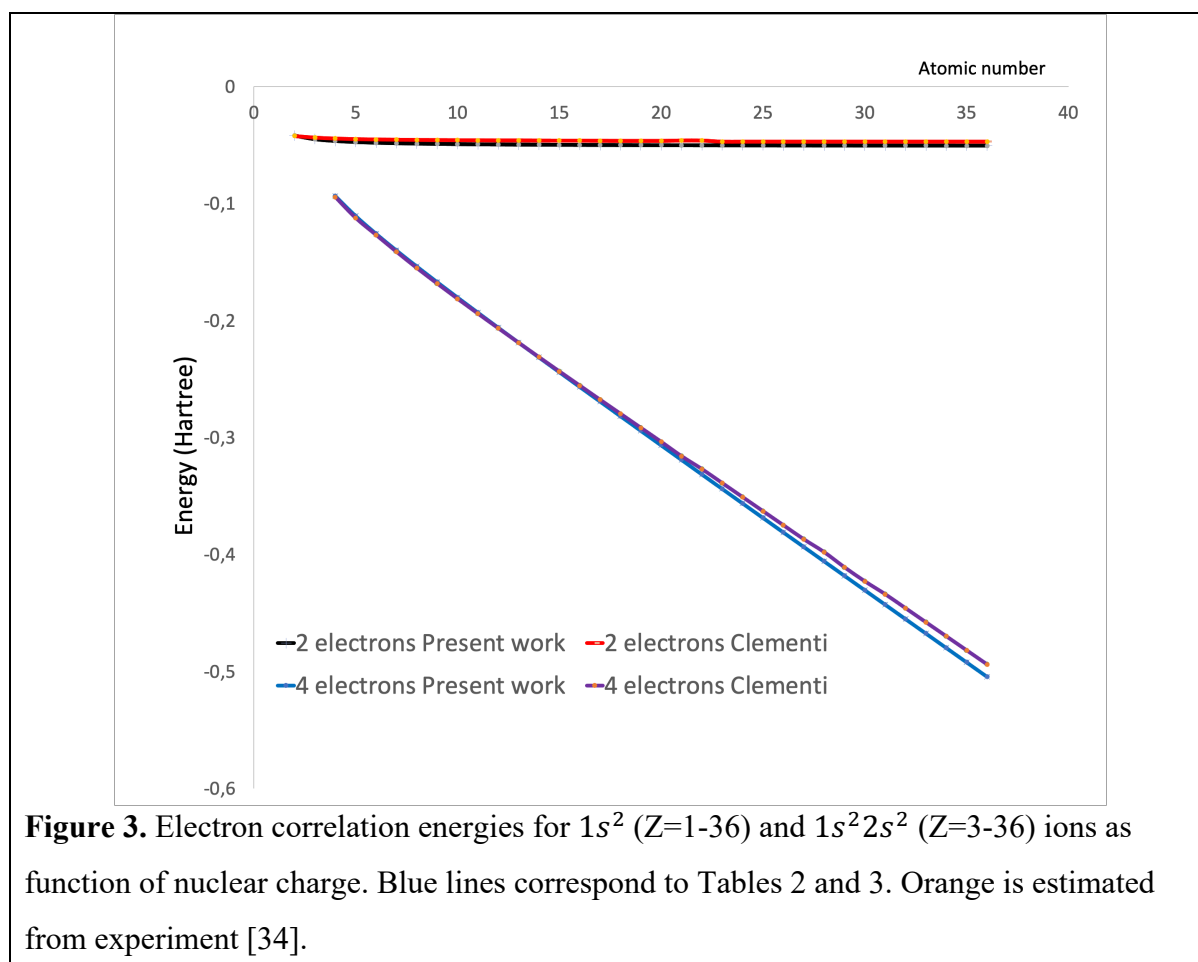


Table 4. Comparison of HF and reg-HF energies for selected ions. Comparisons with accurate HF and explicit electron correlation calculations and estimates in the literature are provided. HGBS-9 basis set [37] is employed in this work.		
Helium		
Descriptions	HF	$E_{tot} \approx reg - HF$
This work	-2.86167999	-2.90337214
Exact: [38]	-2.86167910	-2.90372438
Hydrogen anion		
This work	-0.48792973	-0.51976452
Exact: [38]	-0.48792973	-0.52775101
Lithium mono-cation:		
This work	-7.23641519	-7.28125252
Exact: [38]	-7.23641520	-7.27991341
Lithium anion:		
This work	-7.42820493	-7.49909271
Exact:[39]	-7.42820493	-7.5007512
Beryllium:		
This work	-14.57302313	-14.66640254
Exact:[40]	-14.57302313	-14.66735651

To understand the remaining deviations from the exact value, it should be born in mind that the formalism is based on effective electrons separability and 1st order perturbation theory. Analogous to the V-representability of DFT, it becomes essential that the emerging SCF Slater determinant is a “true” match to the employed $\hat{H}_{effective}$ in the sense of Eq. 11. Systematic deviation is expected when the $f \sim \frac{1}{Z}$ scaling, associated Coulomb hole for the 1s orbital, becomes ill-defined, see HeH^+ and H_3^+ below. To clarify this, consider here the electron affinity of the hydrogen atom, cf. Table 4 again. We find $EA_H^{HF} = -0.33 eV$, $EA_H^{reg-HF} = +0.54 eV$ and $EA_H^{exp} = +0.75 eV$. While significantly improved when

compared to the HF result, disagreement remains with the exact electron affinity. It is the complex three-body nature of that system that limits the reg-HF approach, i.e., the electron correlation renders the electron density subdivided into a more diffuse outer electron density and an inner more hydrogen-like contribution [41]. Indeed, the complexity of the hydride ion is contrasted by Lithium for which $E_{\text{reg-HF}}(\text{Li}^-)$ compares well with $E_{\text{exact}}(\text{Li}^-)$ as does $E_{\text{reg-HF}}(\text{Li}^+)$ with $E_{\text{exact}}(\text{Li}^+)$, cf. Table 4. Analogous agreement with the exact total energy is obtained for the Beryllium atom, cf. Table 4 again. These findings support the notion that beyond hydrogen, the impact of the 1s region reduces to the $f \sim \frac{1}{Z}$ scaling of the Coulomb hole associated with interactions with K-shell electrons, see Eq. 58, Figure 3 and Table 3 again. We conclude that the direct impact of nuclear charge on valence-valence interactions becomes negligible throughout, i.e., $f_V = 1$.

7. Validation II: Small molecules and molecular ions

Modelling in quantum chemistry is generally associated with chemical usefulness.

Consequently, error cancellation becomes central. Here however, we compare total energies to assess the performance of our Coulomb hole model. Resorting to s-type gaussian basis functions, we employ “ghost” basis sets to saturate the description at the Hartree-Fock level. Throughout, our bare Hartree-Fock results should come close to the HF basis set limit, while the reg-HF numbers should compare to the exact values for the correlated systems thereby rendering any shortcomings tractable.

Repeatedly, the efficiency of the reg-HF description of the Coulomb hole is taken to reflect the ability of the Slater determinantal wave function of non-pathological systems to properly truncate the exact wavefunction, cf. Eqs.11-13. Implicit properties that emerge from the stability and assumed validity of the SCF Slater determinant include both implicit electron-electron correlations and molecular structure. In as much as the virial augmented

Coulomb hole constitutes a net attractive contribution to the molecular energy, correspondingly, a virial kinetic energy is understood to maintain the SCF molecular structure. For the systems studied here, the molecular structures predicted by Hartree-Fock theory are often reasonably close to the true values. In general, this agreement is due to the cancellation of two errors, i.e., dynamic correlation tends to shorten bonds while static correlation causes bond elongation. Assuming the V-representability to hold, and both static and dynamic electron correlation to be included in our dressed Coulomb hole, then maintaining any given molecular structure, from Hartree-Fock or other methods, must be associated with a repulsive “kinetic” energy penalty. Because the minimum on the Coulomb hole potential energy surface PES is quadratic in vicinity of its minimum, and $V=-T$ for harmonic potentials, the kinetic energy cost for displacing the nuclei from the Coulomb hole PES minimum to that from the SCF, is exactly accounted for by the electronic virial augmented Coulomb hole formalism. This argument is understood to hold true also if the structures are obtained from experiment or from 1st principles.

In what follows, we present molecular total energies for s-type basis sets. “Ghost” atoms, here even-tempered 7 gaussian s-basis functions starting with gaussian exponents 0.05 void of nuclear charge, are included to add the necessary flexibility to the electronic degrees of freedom. Connection with the Hartree-Fock limit is made to test the internal consistency of the overall understanding. In Table 5, the straight-forward H_2 , LiH , and BeH^+ systems are contrasted somewhat by Li_2 , for incomplete V-representability of the HF wave function, and by HeH^+ and H_3^+ for ill-defined Z-scaling in case of the two latter. Comparisons are made between the analogous expressions Eqs. 50 and 51 to test the robustness of results.

Table 5. Comparison of HF and reg-HF energies for selected molecules. The s-basis sets of HGBS-9 [37] is utilized in conjunction with a geometry optimized even-tempered ghost basis set composed of 7 s-functions. Comparisons with accurate HF and explicit electron correlation calculations and estimates in the literature are provided.

System	Description	E_{HF}	$E_{tot} \approx E_{reg-HF}$	$E_{tot} - E_{HF}$
H_2 $R_{H-H} = 1.40 \text{ au}$ $R_{H-ghost} = \pm 0.21 \text{ au}$	Eq. 50	-1.13362299	-1.17392564	-0.0403027
	Eq. 51		-1.17416125	-0.0405383
	Exact	-1.13362957⁴²	-1.17447^{43,44}	-0.0408444
LiH $R_{Li-H}^{Exp.} = 3.015 \text{ au}$ $R_{Li-ghost} = +0.445 \text{ au}$ $R_{H-ghost} = -0.275 \text{ au}$	Eq. 50	-7.98713813	-8.06559196	-0.0784538
	Eq. 51		-8.06846076	-0.0813226
	Exact	-7.9873646^{45,46}	-8.0705473⁴⁷	-0.0831827
BeH^+ $R_{Be-H} = 2.464 \text{ au}$ $R_{Be-ghost} = 0.286 \text{ au}$ $R_{H-ghost} = -0.208 \text{ au}$	Eq. 50	-14.85351869	-14.93885215	-0.0853334
	Eq. 51		-14.94167398	-0.0881552
	Exact	-14.854177⁴⁸	-14.941822⁴⁹	-0.087645
Li_2 $R_{Li-Li}^{Exp} = 5.05 \text{ au}$ A $R_{Li-ghost} = \pm 0.22 \text{ au}$ B $R_{Li-ghost}(I) = 0.11 \text{ au}$ $R_{Li-ghost}(II) = 0.33 \text{ au}$	A: Eq. 50	-14.87148903	-14.98656025	-0.1150712
	A: Eq. 51		-14.98884386	-0.1173548
	B: Eq. 50	-14.87153654	-14.986350827	-0.1148143
	B: Eq. 51		-14.988607052	-0.1170706
	Exact	-14.87156285⁴⁵	-14.9954^{47,50}	-0.1238 -0.1224⁵¹
HeH^+ $R_{He-H} = 1.455 \text{ au}$ $R_{He-ghost} = 0.2275 \text{ au}$ $R_{H-ghost} = -0.2275 \text{ au}$	Eq. 50; Z = 2	-2.93307816	-2.96755757	-0.0344794
	Eq. 51; Z = 2		-2.96792233	-0.0348442
	Eq. 50; Z = $\frac{3}{2}$		-2.97893302	-0.0458549
	Eq. 51; Z = $\frac{3}{2}$		-2.97929778	-0.0462196
	Exact	-2.93310327⁴⁶	-2.97869074⁵²	-0.0455875
H_3^+ $R_{H-H} = 1.65 \text{ au}$ $R_{H-ghost} = \pm 0.23 \text{ au}$ Along edges of triangle and in center. (Gaussian exponents > 500 omitted)	Eq. 50; Z = 1	-1.30034028	-1.33098024	-0.0306400
	Eq. 51; Z = 1		-1.33162052	-0.0312802
	Eq. 50; Z = $\frac{3}{4}$		--1.34078791	-0.0404476
	Eq. 51; Z = $\frac{3}{4}$		-1.34142819	-0.0410879
	Eq. 50; Z = $\frac{2}{3}$		-1.34557333	-0.04523305
	Eq. 51; Z = $\frac{2}{3}$		-1.34621361	-0.0458733
	Exact	-1.30040014^{45,46}	-1.343863^{53,54}	-0.043463

a. On the H_2 , LiH , and BeH^+ two- and four-electrons systems

Indeed, in as much as electron-nucleus cusp effects are negligible in the valence beyond He, i.e., $f = 1$ for Li 2s and Be 2s, in case of hydrogen where $Z=1$, infers $f \approx 0.987$, which is deemed close to the generic $f = 1$ for valence shells, thus partly explaining the near-perfect results for H_2 , LiH , and BeH^+ . The numerical agreements are taken to suggest that the virial of the systems does indeed include both dynamic and static electron correlation contributions.

b. On the Li_2 and $LiBe^+$ six-electrons systems

The V-representability is commonly understood to be contested somewhat in the 6-electrons system Li_2 . This might be taken to explain the reg-HF total energy underestimation by ~ 0.20 eV, see Table 5 again. Inherently difficult to resolve for several reasons, attempts at estimating the non-dynamic electron correlation by employing CASSCF arrive at 0.71 eV [55]. The latter number would constitute an overestimate, however, as the variational CASSCF method cannot avoid but to also include correlation contributions that are nominally considered dynamic. Still, this would beg to imply that static correlation is to a non-negligible extent accounted for by our exact-exchange reg-HF method. A contrasting aspect to Li_2 is provided from studying the $LiBe^+$ molecular ion, see Table 6. Fortuitous agreement between the CCSDT [56] and HF has been reported for the binding energy, while reg-HF undershoots by ~ 0.2 eV.

Table 6. Comparison of HF, reg-HF and CCSDT [56] results for LiBe⁺. Valence only–reg-HF includes only the valence electrons contribution to the correlation energy.

	Method	Total energy (Ha)	D _e (eV)
LiBe⁺ $R_{Li-Be} = 4.919 \text{ au}$ $R_{Li-ghost(I)} = 0.11 \text{ au}$ $R_{Li-ghost(II)} = 0.33 \text{ au}$ $R_{Be-ghost(I)} = -0.11 \text{ au}$ $R_{Be-ghost(II)} = -0.33 \text{ au}$	HF	-21.83267045	0.63 eV
	CCSDT [56]	-	0.605
	reg-HF		
	Eq. 50	-21.95919862	0.314
	Eq. 51	-21.96272892	0.410
	Valence only – reg-HF		
	Eq. 50	-21.85882621	0.582
Eq. 51	-21.85881364	0.582	
Be	Valence only– reg-HF	-14.60101656	-
Li⁺	Valence only– reg-HF	same as HF (-7.23641519)	-

Here, agreement between the different methods is reached by omitting the core-core and core-valence contributions to the reg-HF energy, while retaining the valence-only contribution, *cf.* Table 6. This infers that the cause for the *a priori* energy difference originates from the 1st order contribution to the energy, i.e., disallowing response in the wave function owing to the core-valence correlation, rather than any absence of static correlation description. This supports the relevance of replacing the K-shells by ECP:s.

c. Possible K-shell chemistry – Comparison of Li⁺, HeH⁺ and H₃⁺ two-electron systems

The complex interplay between electron-nucleus and electron-electron cusps, resulting in Z-screened K-shell Coulomb holes, is a topic on its own. In chemistry, it is often deemed of less importance as practical calculations commonly resort to accurate valence-only descriptions (*cf.* section 6.b and Table 6) as well as ECP:s. For systems like HeH⁺ and H₃⁺, however, dealing with this issue cannot be avoided. The kinship of these three systems (three protons, 2 electrons) was discussed by Banyard et al [57,58]. We note in bypassing how close the exact

electron correlation energy E_{corr}^{exact} come for these systems, i.e., -0.04345 Ha (Li^+), -0.04559 Ha (HeH^+), -0.043463 Ha (H_3^+). Reg-HF predicting 97% of the exact electron correlation energy E_{corr}^{exact} of Li^+ , see Table 4, is deemed satisfactory. Less so for the exotic HeH^+ , where reg-HF ($Z=2$) predicts 75-77% of E_{corr}^{exact} . For this system however, the interplay between short-range electron-nucleus and electron-electron interactions renders the scaling procedure ill-defined. This is because the $1\sigma^2$ orbital in a “unified-atom” sense [59] comes out significantly larger than that of Helium $1s^2$, thus not reflecting the bare charge of the latter. It is gratifying to note that *ad hoc* interpolation between $Z=1$ and $Z=2$ by computing reg – HF ($Z_{eff} = 1.5$) provides 100.5-101.5% of E_{corr}^{exact} . Elaborating further on the inferred exotic K-shell “unified-atoms” chemistry, finally consider the two-electron three-center cluster bond in equilateral triangular H_3^+ . Analogous, yet complementary to the HeH^+ case, here too the interplay between electron-nucleus and electron-electron interactions is understood to be anomalous. Indeed, it suggests the screened Coulomb hole to exhibit $Z_{eff} < 1$. While reg-HF ($Z=1$) captures to some 70% of E_{corr}^{exact} , cf. Table 5 again, it is noted that reg-HF ($Z_{eff} = \frac{3}{4}$) and reg-HF ($Z_{eff} = \frac{2}{3}$) predict 93-94% and 104-106%, respectively. This feature is understood to have bearing on the modelling of solid and liquid hydrogen at high pressures [60].

8. Summary and Conclusions

The notion that the electron correlation energy conceptually comprises an inherent property of Hartree-Fock theory was developed.

1. A self-interaction-free exact-exchange method that accurately estimates E_{corr} emerges as 1st order correction to the Hartree – Fock energy was deduced and validated.

2. Building on the virial theorem, the Coulomb hole augmented effective Hamiltonian is valid on condition of stability of the SCF wave function. Consequently, the formalism evolved from damping out the short-range contribution to the electron repulsion operator, replacing it by the corresponding correlation kinetic energy penalty.
3. The coupling of electron-nucleus and electron-electron interactions in the K-shell, absent when Effective Core Potentials are employed, was accounted for by scaling the Coulomb holes that explicitly involve 1s orbitals by the proximal nuclear charges.
4. Hooke's atom was employed to parametrize the screening of the dressed coulomb hole by the bare nuclear charges in cases of interactions with K-shell electrons.
5. For $1s^2$ systems, consistency was demonstrated in case of (a) Hooke's atom for a range of different force constants, and (b) He-like ions for $Z=1-36$.
6. For the valence-valence interactions other than among K-shell orbitals, the screening of the Coulomb hole owing to the short-range electron-nucleus interaction vanishes as validated by the Be-like ions $Z=3-36$ $1s^2 2s^2$ systems, as well as by the molecular LiH, BeH^+ , Li_2 and LiBe^+ .
7. A chemistry associated exclusively with K-shell orbitals was briefly discussed based mainly on results for HeH^+ and H_3^+ . Fractional charge augmenting the Coulomb hole was inferred to better represent the complex correlation hole in hydrogen clusters and high-pressure metallic hydrogen.
8. The procedure for transferring the electron correlation property from the wave function into the electron repulsion operator is applicable to the same class of systems as DFT. Indeed, it may serve as inspiration in the development of new and improved classes of self-interaction-free exact-exchange and hybrid functionals.
9. The handy Laplace and Fourier transforms of the virial augmented regularized electron repulsion operator ensure usefulness irrespective of whether gaussian or

plane-wave bases – or a combination of the two – are used for spanning the electronic orbitals. This is understood to facilitate implementations for solid state applications.

10. While this regularized Hartree-Fock method is found to perform well overall, still, literature [12,29] estimates $E_{corr}(He - like) = 1.28$ eV for $Z \rightarrow \infty$, while reg-HF predicts 1.38 eV. Analogously, $E_{corr}(Hooke) = 1.35$ eV was deduced for $\omega \rightarrow \infty$ [61], while reg-HF predicts 1.25 eV. This is explained by the perturbative nature of the regularized Hartree-Fock approach.

The success of the reg-HF approach is attributed to better obeying the Heisenberg indeterminacy principle [2], a property that is exclusive to the exact wave function. It is achieved by disallowing the representation of the electron repulsion operator to be more fine-grained than the corresponding representation of the two-particle density.

Computational details

Mathematica [62] was used for the plots in Figures 1 and 2. A MATLAB [63] code was written to solve for Roothaan's equations [11], as well as for the present regularized Hartree-Fock scheme. Figure 3 was made in Microsoft Excel.

References

1. Schrodinger, E. Quantisierung als Eigenwertproblem. *Annalen der Physik* **1926**, *384*, 361-376.
2. Heisenberg, W. Über den anschaulichen Inhalt der quantentheoretischen Kinematik und Mechanik, *Zeitschrift für Physik*. **1927**, *43*(3–4): 172–198.
3. von Neumann, J. Mathematical Foundations of Quantum Mechanics. **1955**, *Princeton University Press*, Princeton.
4. Shannon, C. E. "A mathematical theory of communication," in *The Bell System Technical Journal*, **1948**, *27*(4), 623-656.
5. Hartree, D. The Wave Mechanics of an Atom with a Non-Coulomb Central Field. Part II. Some Results and Discussion. *Mathematical Proceedings of the Cambridge Philosophical Society* **1928**, *24*(1), 111-132.
6. Slater, J. C. The Self Consistent Field and the Structure of Atoms, *Phys. Rev.* **1928**, *32* (3), 339-348.
7. Gaunt, J. A Theory of Hartree's Atomic Fields. *Mathematical Proceedings of the Cambridge Philosophical Society* **1928**, *24*(2), 328-342.
8. Slater, J. C. Note on Hartree's method, *Phys. Rev.* **35** (2), 210 (1930).
9. Fock, V. Näherungsmethode zur Lösung des quantenmechanischen Mehrkörperproblems. *Z. Physik* **1930**, *61*, 126–148
10. Hartree, D.R.; Hartree, W. Self-consistent field, with exchange, for beryllium, *Proc. Royal Soc. Lond.* **1935**, *A150*,, 9-33.
11. Roothaan, C. C. J. New Developments in Molecular Orbital Theory, *Reviews of Modern Physics* **1951**, *23* (2): 69-89.
12. Löwdin, P.-O. Scaling problem, virial theorem, and connected relations in quantum mechanics, *J. Molecular Spectroscopy* **1959**, *3* (1-6), 46-66
13. Hylleraas, E. A. Neue Berechnung der Energie des Heliums im Grundzustande, sowie des tiefsten Terms von Ortho-Helium, *Z. Phys.* **1929**, *54*, 347-366
14. Löwdin, P.-O. Correlation Problem in Many-Electron Quantum Mechanics I. Review of Different Approaches and Discussion of Some Current Ideas. In *Advances in Chemical Physics*, **1958** Prigogine, I. (Ed.).
15. Kutzelnigg, W. r_{12} -Dependent terms in the wave function as closed sums of partial wave amplitudes for large l . *Theoret. Chim. Acta* **1985**, *68*, 445–469.

16. Kutzelnigg, W. and Klopper, W. Wave functions with terms linear in the interelectronic coordinates to take care of the correlation cusp. I. General theory, *J. Chem. Phys.* **1991**, *94*, 1985-2001.
17. Slater, J. C. Future Prospects for the X α Method, *Int. J. Quantum. Chem. Symp.* **1973** *7*, 533-544.
18. Clementi, E.; Hofmann, D.W.M. Coulomb-Hole–Hartree–Fock functional. *Int. J. Quantum Chem.* **1994**, *52*, 849-865.
19. Hohenberg, P.; Kohn, W. Inhomogeneous Electron Gas, *Phys. Rev.* **1964**, *136*, 864-871.
20. Kohn, W.; Sham, L.J. Self-Consistent Equations Including Exchange and Correlation Effects, *Physical Review* **1965**, *140 (4A)*, 1133-1138
21. Panas, I. Aspects of density functional theory in ab initio quantum chemistry: external correlation for free, *Chem. Phys. Letters* **1995**, *245 (2-3)*. 171-177
22. Panas, I. A Coulomb hole approach to the binding in Cr₂, *Molecular Physics* **1996**, *89:1*, 239-246.
23. Panas, I.; Snis, A. Effective dynamic correlation in multiconfigurational wave-function calculations on atoms and molecules. *Theor Chem Acta* **1997**, *97*, 232–239.
24. Cizek, J.; Paldus, J. *Intern. J. Quantum Chem.* **5** (1971) 359.
25. Harris, F.E. *Intern. J. Quantum Chem. Symp.* **11** (1977) 403.
26. Bartlett R.J.; Purvis, G.D. *Intern. J. Quantum Chem.* **1978**, *16*, 561.
27. Jørgensen, P; Simon, J. Second quantization-based methods in quantum chemistry (Academic Press, New York, 1981)].
28. Slater, J. C. The Virial and Molecular Structure, *J. Chem. Phys.* **1933**, *1*, 687-691.
29. Fröman, A. Correlation Energies of Some He- and Ne-Like Systems, *Phys. Rev.* **1958**, *112*, 870-872.
30. Levy, M.; Perdew, J. P., Hellmann-Feynman, virial, and scaling requisites for the exact universal density functionals. Shape of the correlation potential and diamagnetic susceptibility for atoms, *Phys. Rev.* **1985**, *A32*, 2010-2021.
31. Kestner, N. R.; Sinanoglu, O., Study of Electron Correlation in Helium-Like Systems Using an Exactly Soluble Model, *Phys. Rev.* **1962**, *128*, 2687—2692.
32. Taut, M. Two electrons in an external oscillator potential: Particular analytic solutions of a Coulomb correlation problem, *Phys. Rev.* **1993** *A48*, 3561—3566.

33. O'Neill, D. P.; Gill, P. W. M. Wave functions and two-electron probability distributions of the Hooke's-law atom and helium, *Phys. Rev.* **2003**, *A68*, 022505.
34. Matito, E.; Cioslowski, J.; Vyboishchikov, S. F. *Phys. Chem. Chem. Phys.*, **2010**, *12*, 6712-6716.
35. Benson, J. M.; Byers Brown, W. Perturbation Energies for the Hooke's Law Model of the Two-Electron Atom, *J. Chem. Phys.* **1979**, *53*, 3880-3886.
36. Clementi, E. Correlation Energy for Atomic Systems, *J. Chem. Phys.* **1963**, *38*, 2248-2256.
37. Lehtola, S. Polarized Gaussian basis sets from one-electron ions, *J. Chem. Phys.* **2020**, *152*, 134108.
38. Baskerville, A. L.; King, A. W.; Cox, H. Electron correlation in Li^+ , He, H_2 and the critical nuclear charge system ZC: energies, densities and Coulomb holes. *R. Soc. open sci.* **2019**, *6*, 181357.
39. Chung, K. T.; Fullbright, P. Electron affinity of lithium, *Phys. Scr.* **1992**, *45*, 445-449.
40. Hornyák, I.; Adamowicz, L.; Bubin, S. Ground and excited s^1 states of the beryllium atom, *Phys. Rev.* **2019**, *A100*, 032504.
41. Banyard, K. E. Correlation of Electrons Within the Hydride Ion, *J. Chem. Phys.* **1968**, *48*, 2121-2129.
42. Jensen, F. The basis set convergence of the Hartree–Fock energy for H_2 , *J. Chem. Phys.* **1999**, *110*, 6601-6605.
43. Kolos, W.; Wolniewicz, L. Improved Theoretical Ground-State Energy of the Hydrogen Molecule, *J. Chem. Phys.* **1968**, *49*, 404-410.
44. Wright, J. S.; Barclay, V. J. Approaching the exact energy for H_2 : Bond functions vs polarization functions, *J. Chem. Phys.* **1987**, *86*, 3054-3055.
45. Jensen, F. The basis set convergence of the Hartree–Fock energy for H_3^+ , Li_2 and N_2 . *Theor Chem Acc* **2000**, *104*, 484–490.
46. Tasi, G.; Csaszar, A. G. Hartree–Fock-limit energies and structures with a few dozen distributed Gaussians, *Chem. Phys. Letters* **2007**, *438* (1-3) 139-143.
47. Nasiri, S.; Zahedi, M. Accurate potential energy curves of Li_2 and LiH : A Quantum Monte-Carlo (QMC) study, *Chem. Phys. Letters.* **2015**, *634*, 101-107.
48. Pyykkö, P.; Sundholm, D.; Laaksonen, L. (1987) Two-dimensional, fully numerical molecular calculations, *Molecular Physics* **1987**, *60*:3, 597-604.
49. Koput, J. Ab initio ground-state potential energy functions of beryllium monohydride ions: BeH^+ and BeH^- , *J. Chem. Phys.* **2013**, *139*, 104309.

50. Filippi, C.; Umrigar, C. J. Multiconfiguration wave functions for quantum Monte Carlo calculations of first-row diatomic molecules, *J. Chem. Phys.* **1996**, *105*, 213-226.
51. Freeman, D. L.; Karplus, M., Many-body perturbation theory applied to molecules: Analysis and correlation energy calculation for Li₂, N₂, and H₃, *J. Chem. Phys.* **1976**, *64*, 2641-2659.
52. Dou, Y., Tang, H. & Bai, M. Molecular calculations for HeH⁺ with two-center correlated orbitals. *Sci. China Ser. B-Chem.* **2009**, *52*, 2249.
53. Cencek, W.; Komasa, J.; Rychlewski, J. Benchmark calculations for two-electron systems using explicitly correlated Gaussian functions, *Chem. Phys. Lett.* **1995**, *246* (4-5), 417-420.
54. Pavanello, M.; Adamowicz, L. High-accuracy calculations of the ground, 1A1'11 A11', and the 2A1'12 A11', 2A3'12 A31', and 1E1'1 E1' excited states of H₃⁺, *J. Chem. Phys.* **2009**, *130*, 034104.
55. Mok, D K. W; Neumann, R.; Nicholas C. Handy, N. C. Dynamical and Nondynamical Correlation, *The Journal of Physical Chemistry* **1996**, *100* (15), 6225-6230.
56. Fedorov, D. A.; Barnes, D. K.; Varganov, S. A. Ab initio calculations of spectroscopic constants and vibrational state lifetimes of diatomic alkali-alkaline-earth cations, *J. Chem. Phys.* **2017**, *147*, 124304.
57. Banyard, K. E.; Baker, C. C. Molecular formation and electron correlation in HeH⁺, *Int. J. Quant. Chem.* **1970**, *4*, 431-450.
58. Banyard, K. E.; Sanders, J. The H₃⁺ molecule ion: A two-particle density study of electron correlation, *J. Chem. Phys.* **1994**, *101*, 3096-3103.
59. Pack, R. T.; Byers Brown, W. Cusp Conditions for Molecular Wavefunctions, *J. Chem. Phys.* **1966**, *45*, 556-559.
60. Celliers; P. M.; Millot, M.; Brygoo, S., McWilliams, R.S.; et al. Insulator-metal transition in dense fluid deuterium. *Science*. **2018**, *361* (6403), 677-682.
61. Gill, P. M. W.; O'Neill, D. P. Electron correlation in Hooke's law atom in the high-density limit, *J. Chem. Phys.* **2005**, *122*, 094110.
62. Mathematica Version 13.1, Wolfram Research, Inc.
63. MATLAB R2022b.